NH, respectively.[15,16] Except for the presence of exchangeable proton resonances, the spectrum is very similar but not quite identical with that reported in ^2H_2O.[14] In a 50:50 mixture of ^1H_2O and ^2H_2O (Figure 1B), the spectrum corresponds to a 1:1 superposition of the subspectra recorded in the isotopically pure solvents. It is obvious that most but not all nonexchangeable proton signals coincide: the three heme methyl peaks yield double lines as shown in the expansion of Figure 1B. The relative splittings of the 5-, 1-, and 8-methyl peaks are 32, 16, and 18 Hz, respectively. Thus, the isotope composition of the solvent exerts an influence on the electronic structure of the heme, and the two species differentiated by the solvent isotopes are in slow exchange on the NMR time scale ($<<2 \times 10^2$ s^{-1}) at 30 °C and pH 9.2.

The response of the two 5-methyl peak intensities to variable solvent isotope composition is illustrated by the three ^1H_2O:^2H_2O ratios shown in Figure 2: 90:10 (A), 70:30 (B), and 50:50 (C). In any solvent mixture, there are two and only two lines per heme methyl group, and their relative intensity is identical with the bulk ^1H:^2H solvent composition. This immediately allows the conclusion that *the isotope perturbation on the heme electronic structure is due exclusively to a single $^1H/^2H$ exchange site in the protein.* The low field component for each heme methyl corresponds to the "^1H" form, while the high field component arises from the "^2H" form in each case. Splittings for other resonances are not resolved.

Logical candidates for this unprecedented isotope effect on the heme electronic structure are heme cavity labile protons: proximal His ring or peptide protons (*B* or *C*) and distal His ring proton (*A*). Specific assignment can be effected on the basis of the known exchange rates for *A*, *B*, and C.[16] When the bound ^1H or ^2H exchanges with bulk solvent at a rate much faster than the chemical shift separation, the two subspectra must coalesce into one averaged spectrum. The effect of pH at 30 °C is displayed in traces D–G of Figure 2, which demonstrate that the dynamic collapse of the two 5-methyl signals is acid-catalyzed. Furthermore, the lines remain well-resolved and sharp up to pH 10.4. Only the distal His ring NH exhibits a compatible exchange behavior.[16] With use of the equation for a two-site exchange process,[17] analysis of the line width of the collapsed line at pH 7.24 yields an exchange rate of $\sim 10^2$ s^{-1}, which is of the order of that determined for the distal His ring NH by saturation transfer from bulk solvent.[16,18] Differential paramagnetic relaxation has already demonstrated that the His E7 ring (peak *A*) must be within 4.2 Å of the iron and thus close to the bound cyanide.[16]

We conclude that the perturbation of the heme electronic structure arises directly from the isotope effect of the H bond between the distal His E7 and the bound ligand.[19] Since such an H bond is present in MbO_2[8] and absent in MbCO,[20] our NMR data indicate that, regarding distal interactions, cyanide is a better model for O_2 than for CO, even though the conformational tendencies of CN^- more closely resemble that of CO. The relative magnitudes of the isotope splitting and the fact that only heme resonances exhibit such splitting demand that the contact, and not the dipolar, contribution[13] to the hyperfine shift be sensitive to the $^1H/^2H$ replacement. Since the resolved "^1H" heme methyl shifts are all downfield of the "^2H" components, it appears that the heme in-plane asymmetry is larger in ^1H_2O than in ^2H_2O. The observed shifts confirm the direct influence of the distal ligand on the heme electronic structure and provides important evidence for its contribution to the asymmetry of the unpaired spin distribution.[13,21] This can be rationalized by the observation that the CN^- is tilted from the heme normal[5] and suggests that the differential $^1H/^2H$ bonding either induces an electronic perturbation in the Fe–CN bond or causes a small change in tilt angle. The absence of an isotope effect on the bound cyanide stretching frequencies in metMbCN[5] favors the latter interpretation. The effect of H bonding on the heme methyl contact shift pattern requires reassessment of the simple picture where only the proximal imidazole orientation modulates the in-plane asymmetry.[21] A more quantitative interpretation awaits the availability of a suitable X-ray structure of metMbCN.

The observation of similar, but highly differential, solvent isotope splittings of heme resonances in a variety of ferric cyanide ligated derivatives of other myoglobins, hemoglobins, and peroxidases indicates that the present NMR method provides a new probe of H bonding in heme proteins which will have broad applicability.

Acknowledgment. This study was supported by a grant from the National Institutes of Health, HL-16087. We are indebted to S. W. Unger for experimental assistance.

(15) Sheard, B.; Yamane, T.; Shulman, R. G. *J. Mol. Biol.* **1970**, *53*, 35–48.
(16) Cutnell, J. D.; La Mar, G. N.; Kong, S. B. *J. Am. Chem. Soc.* **1981**, *103*, 3567–3572.
(17) Sandström, J. In *Dynamic NMR Spectroscopy*; Academic Press: London, 1982; Chapter 2.
(18) Saturation transfer data as reported in ref 16 also predict a rate of exchange slower than 5 s^{-1} at pH 9.2. Such a slow rate introduces essentially no broadening[17] of the individual 5-methyl lines whose widths in the pure solvents are ~35 Hz.
(19) To ascertain that the effect is not due to His 97 (FG3) or Arg 45 (CD3), which are H bonded to the 7- and 6-heme propionates, respectively (Takano, T. *J. Mol. Biol.* **1977**, *110*, 537–568; 569–584), we used 6-(2-carboxyethyl)-1,3,5,7,8-pentamethyl-2,4-divinylhemin-reconstituted metMbCN (La Mar, G. N.; Emerson, S. D.; Lecomte, J. T. J.; Pande, V.; Smith, K. M.; Craig, G. W.; Kehres, L. A. *J. Am. Chem. Soc.* **1986**, *108*, 5568–5573) (no H bond to His 97) and horse metMbCN (Ar 45 → Lys 45, Dayhoff, M. O. *Atlas of Protein Sequence and Structure*; National Biomedical Research Foundation: Washington, DC 1972; Vol. 5). At pH 9.2, the splitting of the heme methyl line is, in both cases, identical with that of native sperm whale metMbCN.
(20) Norvel, J. C.; Nunes, A. C.; Schoenborn, B. P. *Science (Washington, D. C.)* **1975**, *190*, 568–570.
(21) (a) Shulman, R. G.; Glarum, S. H.; Karplus, M. *J. Mol. Biol.* **1971**, *57*, 93–115. (b) Traylor, T. G.; Berzinis, A. P. *J. Am. Chem. Soc.* **1980**, *102*, 2844–2846.

Structures of the New Binary Metal Carbonyl $Os_4(CO)_{15}$ and $(\eta^5\text{-}C_5Me_5)(OC)IrOs_3(CO)_{11}$. Clusters with Three-Center–Two-Electron Metal–Metal Bonds?

Victor J. Johnston, Frederick W. B. Einstein,* and Roland K. Pomeroy*

Department of Chemistry, Simon Fraser University Burnaby, British Columbia, Canada V5A 1S6

Received June 16, 1987

Of the transition metals, osmium forms the most neutral binary carbonyls. The crystal structures of $Os_3(CO)_{12}$,[1] $Os_5(CO)_{16}$,[2] $Os_5(CO)_{19}$,[3] $Os_6(CO)_{18}$,[4] $Os_7(CO)_{21}$,[5] and $Os_8(CO)_{23}$[6] have been determined. Pentacarbonylosmium, $Os(CO)_5$,[7] and nonacarbonyldiosmium, $Os_2(CO)_9$,[8] are also known as is $Os_6(CO)_{21}$, previously considered to be $Os_6(CO)_{20}$.[3,9] However, to our knowledge there are no previous reports of a tetranuclear binary

(1) Churchill, M. R.; DeBoer, B. G. *Inorg. Chem.* **1977**, *16*, 878.
(2) Eady, C. R.; Johnson, B. F. G.; Lewis, J.; Reichert, B. E.; Sheldrick, G. M. *J. Chem. Soc., Chem. Commun.* **1976**, 271.
(3) Farrar, D. H.; Johnson, B. F. G.; Lewis, J.; Raithby, P. R.; Rosales, M. J. *J. Chem. Soc., Dalton Trans.* **1982**, 2051.
(4) Mason, R.; Thomas, K. M.; Mingos, D. M. P. *J. Am. Chem. Soc.* **1973**, *95*, 3802.
(5) Eady, C. R.; Johnson, B. F. G.; Lewis, J.; Mason, R.; Hitchcock, P. B.; Thomas, K. M. *J. Chem. Soc., Chem. Commun.* **1977**, 385.
(6) Jackson, P. F.; Johnson, B. F. G.; Lewis, J.; Nelson, W. J. H.; Pearsall, M. A.; Raithby, P. R.; Vargas, M. D. *J. Chem. Soc., Dalton Trans.*, in press. See: Vargas, M. D.; Nicholls, J. N. *Adv. Inorg. Chem. Radiochem.* **1986**, *30*, 123.
(7) (a) Calderazzo, F.; L'Eplattenier, F. *Inorg. Chem.* **1967**, *6*, 1220. (b) Rushman, P.; van Buuren, G. N.; Shiralian, M.; Pomeroy, R. K. *Organometallics* **1983**, *2*, 693.
(8) Moss, J. R.; Graham, W. A. G. *J. Chem. Soc., Dalton Trans.* **1977**, 95.
(9) Goudsmit, R. J.; Jeffrey, J. G.; Johnson, B. F. G.; Lewis, J.; McQueen, R. C. S.; Sanders, A. J.; Liu, J.-C. *J. Chem. Soc., Chem. Commun.* **1986**, 24.

0002-7863/87/1509-7220$01.50/0

carbonyl of osmium. Given the stability of $Os_3(CO)_{12}$ and allowing for the increase in nonbonded interactions, one might expect that $Os_4(CO)_{16}$ with a square arrangement of metal atoms would be stable. Here we report the synthesis and structure of $Os_4(CO)_{15}$ the first tetranuclear binary carbonyl of osmium, along with the synthesis and structure of $(\eta^5\text{-}C_5Me_5)(OC)IrOs_3(CO)_{11}$. These clusters have unusual planar skeletons with adjacent short and long metal–metal bonds. We have previously observed this configuration of metal atoms in $Os_4(CO)_{14}(PMe_3)$ and have rationalized it in terms of three-center–two-electron metal–metal bonds.[10]

Pentacarbonylosmium (or $(\eta^5\text{-}C_5Me_5)Ir(CO)_2$) does not displace acetonitrile from $Os_3(CO)_{11}(CH_3CN)$, one of the methods used to prepare $Os_3(CO)_{11}[Os(CO)_4(PMe_3)]$ and hence $Os_4(CO)_{14}(PMe_3)$.[10] However, treatment of the cyclooctene derivative $Os_3(CO)_{10}(C_8H_{14})_2$[11] in hexane with an approximately equimolar amount of $Os(CO)_5$ in hexane at room temperature or below readily yields $Os_4(CO)_{15}$ (**1**) as air-stable, dark red crystals.[12] The structure of **1**[13] was determined at −73 °C; a view of the molecule is shown in Figure 1. The Os_4 unit is essentially planar (the dihedral angle between the planes Os(1)–Os(2)–Os(3) and Os(1)–Os(2)–Os(4) is 179.0°). The unit has adjacent short (Os(1)–Os(3) = 2.772 (1) Å; Os(1)–Os(4) = 2.772 (1) Å) and long (Os(2)–Os(3) = 2.997 (1) Å; Os(2)–Os(4) = 2.997 (1) Å) bonds. Although somewhat long, the diagonal Os(1)–Os(2) bond length at 2.948 (1) Å is more typical of an Os–Os single bond. (In $Os_3(CO)_{12}$, the average Os–Os bond length is 2.877 (3) Å.[1]) As discussed for $Os_4(CO)_{14}(PMe_3)$[10] we believe these unusual bond lengths are best rationalized in terms of three-center–two-electron metal–metal bonds as shown. In this way the Os(1)–Os(3) and

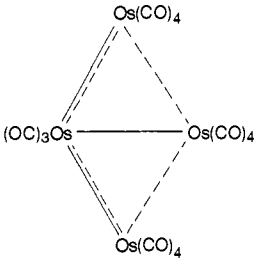

Os(1)–Os(4) bonds are assigned a bond order of 1.5, the Os(2)–Os(3) and Os(2)–Os(4) bonds an order of 0.5, and achieves an 18-electron configuration for each metal atom. (Molecular orbital calculations are in progress in an attempt to support this interpretation.) The cluster is the missing member of the series of $Os_3(CO)_{12}$ and the higher nuclearity planar clusters of osmium such as $Os_5(CO)_{19}$[3] and $Os_6(CO)_{17}[P(OMe)_3]_4$.[9,14]

The osmium–iridium cluster $(\eta^5\text{-}C_5Me_5)(OC)IrOs_3(CO)_{11}$ (**2**)[15] was prepared in a similar manner to **1** from $Os_3(CO)_{10}(C_8H_{14})_2$ and $(\eta^5\text{-}C_5Me_5)Ir(CO)_2$.[16] The crystal structure,[17] determined at room temperature, reveals (Figure 2) an almost planar $IrOs_3$ framework (the dihedral between the planes Os(1)–Os(2)–Ir and Os(1)–Os(2)–Os(3) is 169.9°). Once again, there are adjacent short and long metal–metal bonds: Os(1)–Ir = 2.703 (2) Å, Os(1)–Os(3) = 2.796 (2) Å; Os(2)–Ir = 2.939 (2) Å; Os(2)–Os(3) = 2.994 (2) Å. The diagonal Os–Os bond length (Os(1)–Os(2)) is 2.909 (2) Å. As discussed for **1**, the short and long bonds are consistent with the assignment of bonds of order 1.5 between Os(1)–Ir and Os(1)–Os(3) and of order 0.5 between Os(2)–Ir and Os(2)–Os(3). (Unbridged single Ir–Os bonds reported in the literature range from 2.776 (5) to 2.881 (1) Å.[18] In view of the ability of $(\eta^5\text{-}C_5Me_5)Ir(CO)_2$ to react with hydrocarbons[19] it will be of interest to see if **2** can also bring about C–H activation.

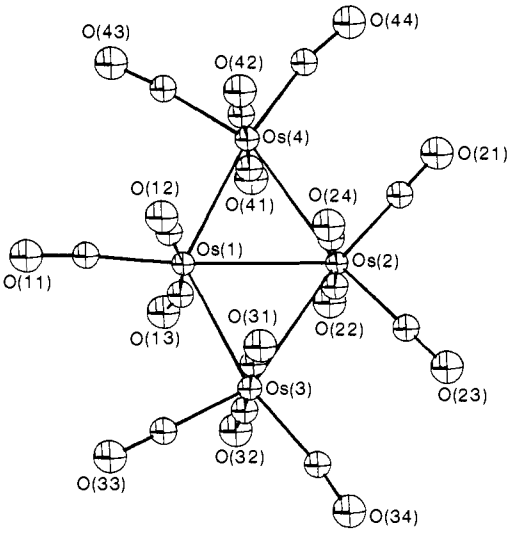

Figure 1. Molecular structure of $Os_4(CO)_{15}$ (**1**).

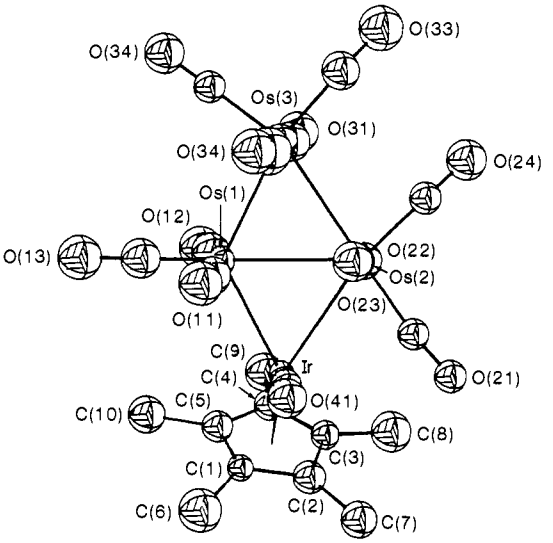

Figure 2. Molecular structure of $(\eta^5\text{-}C_5Me_5)(OC)IrOs_3(CO)_{11}$ (**2**).

(10) Martin, L. R.; Einstein, F. W. B.; Pomeroy, R. K. *J. Am. Chem. Soc.* **1986**, *108*, 338. Martin et al. *Organometallics*, in press.

(11) Tachikawa, M.; Shapley, J. R. *J. Organomet. Chem.* **1977**, *124*, C19.

(12) Isolated yield = 72%. IR ν(CO) (CH_2Cl_2) 2086 (s), 2073.5 (m), 2045 (vs), 2023 (m), 2002 (sh) 1939 (m, br) cm^{-1}; MS, *m/e* 1182 (w) (M^+), 1154 (s) ($[M - CO]^+$). Anal. Calcd for $C_{15}O_{15}Os_4$: C, 15.26; H, 0.0. Found: C, 15.51; H, 0.0.

(13) X-ray diffraction data (−73 °C) for $Os_4(CO)_{15}$: M_r = 1180.8; monoclinic; space group $C2/c$; a = 12.802 (3) Å, b = 10.217 (3) Å, c = 16.380 (5) Å, β = 91.39 (2)°; V = 2141.7 Å^3; Z = 4, D_{calcd} = 3.662 g cm^{-3}; (an analytical absorption correction was applied); diffractometer, Enraf-Nonius CAD4F; radiation, Mo Kα_1 graphite monochromator (λ(Kα_1) = 0.709 30 Å); scan range = 0° ≤ 2θ ≤ 50°; reflections = 1204 with $I_o \geq 2.5\sigma I_o$; R_f = 0.0441, R_w = 0.0537. Our model of the structure consists of two overlapping disordered molecules (each of half occupancy) related by the twofold axis. The number of variables (108) was severely limited, and the model was also restrained to meet reasonable geometrical criteria. Despite these restrictions the agreement was markedly superior to the best ordered model developed in the noncentric space group Cc (R = 0.0522; 120 variables).

(14) Goudsmit, R. J.; Johnson, B. F. G.; Lewis, J.; Raithby, P. R.; Whitmire, K. H. *J. Chem. Soc., Chem. Commun.* **1982**, 640.

(15) IR ν(CO) (hexane) 2107.5 (m), 2075.5 (w), 2062.5 (s), 2038.5 (sh), 2029 (vs), 2021, (sh), 2008 (m), 1987 (w), 1964 (w), 1952.5 (vw), 1934.5 (w), 1927.5 (w) cm^{-1}; MS, *m/e* 1206 ($[M - CO]^+$); ^{1}H NMR ($CDCl_3$) δ 2.03. Anal. Calcd for $C_{22}H_{15}IrO_{12}Os_3$: C, 21.40; H, 1.22. Found: C, 21.50; H, 1.15.

(16) Kang, J. W.; Mosely, K.; Maitlis, P. M. *J. Am. Chem. Soc.* **1969**, *91*, 5970.

(17) X-ray diffraction data for $(\eta^5\text{-}C_5Me_5)(OC)IrOs_3(CO)_{11}$: M_r = 1233.8; monoclinic; space group $P2_1/n$; a = 14.598 (5) Å, b = 20.217 (3) Å, c = 9.084 (3) Å, β = 91.07 (3)°; V = 2667.1 Å^3; Z = 4, D_{calcd} = 3.058 g cm^{-3}; (an analytical absorption correction was applied); diffractometer, Enraf-Nonius CAD4F; radiation, Mo Kα_1 graphite monochromator (λ(Kα_1) = 0.709 30 Å); scan range = 0° ≤ 2θ ≤ 45°; reflections = 2013 with $I_o \geq 2.5\sigma I_o$; R_f = 0.0429, R_w = 0.0457.

(18) Johnson, B. F. G.; Lewis, J.; Raithby, P. R.; Azman, S. N.; Syed-Mustaffa, B.; Taylor, M. J.; Whitmire, K. H.; Clegg, W. *J. Chem. Soc., Dalton Trans.* **1984**, 2111 and references therein.

(19) Hoyano, J. K.; McMaster, A. D.; Graham, W. A. G. *J. Am. Chem. Soc.* **1983**, *105*, 7190.

Acknowledgment. We are grateful to the Natural Sciences and Engineering Research Council of Canada for financial support.

Supplementary Material Available: Tables of atomic coordinates, temperature factors, and bond lengths and angles for **1** and **2** (7 pages). Ordering information is given on any current masthead page.

Microwave Spectrum and Structure of the Trimethylamine–Sulfur Dioxide Charge-Transfer Complex[1]

Marabeth S. LaBarge, José Matos, Kurt W. Hillig II, and Robert L. Kuczkowski*

Department of Chemistry, University of Michigan Ann Arbor, Michigan 48109

Received July 27, 1987

It has been pointed out by Tamres[2] and others[3] that trimethylamine–sulfur dioxide (TMA·SO_2) is the only charge-transfer complex for which the reaction thermodynamics are known in both solution and gas phase as well as the solvation and lattice energies necessary to complete the cycle.[3-5] Its dipole moment[6] and matrix IR spectrum[7] have been reported. Ab initio calculations gave N–S distances of 2.86[8] and 2.36 Å[9] compared with 2.06 Å by X-ray crystallography.[10] The SO_2 plane reportedly makes an angle with the TMA symmetry axis of 90–95° in the theoretical studies and 112° in the crystallographic study, with the sulfur atom close to the TMA axis. A 90° approach is not expected for a dipolar interaction but is favored when higher order electrostatic terms are considered.[11]

Such charge-transfer complexes have not been studied by conventional microwave spectroscopy due to the complexity of typical systems and their small equilibrium concentrations at low pressures. We have recently observed the rotational spectrum of TMA·SO_2 formed in a supersonic expansion using a Fourier-transform microwave (FTMW) spectrometer.[12,13] This has provided some insight on the structure of the complex.

A TMA·SO_2 sample[14] was held at 75–125 °C in a small chamber attached to a modified Bosch fuel injector pulsed valve. The equilibrium vapor above the sample (about 99% dissociated TMA·SO_2) was mixed with 1–2 atm of argon and pulsed through a 1-mm orifice into the resonant cavity of the FTMW spectrometer. Transitions were observed split by the ^{14}N quadrupole interaction. Components (64) from 18 μ_a and μ_c transitions involving J's between 1 and 4 were fit with an RMS deviation of 2.6 kHz. A weaker set of transitions were found in the regions expected for the ^{34}S species (4% abundance), and 31 components from 10 transitions were similarly fit. No evidence of internal rotation or inversion motions was seen. The spectral constants and selected inertial parameters are listed in Table I. The transition data are available as Supplementary Material.

Table I. Spectroscopic Constants for TMA·SO_2

	TMA·$^{32}SO_2$[a]	TMA·$^{34}SO_2$	free TMA, SO_2[b]
A, MHz	3179.789 (6)	3172.628 (50)	
B, MHz	1720.319 (1)	1703.240 (3)	
C, MHz	1503.603 (1)	1492.122 (2)	
$I_a + I_c - I_b$, amu·Å^2	201.2752	201.2778	199.63
χ_{aa}, MHz	−3.52 (1)	−3.43 (3)	−5.47 (3)
χ_{bb}, MHz	1.96 (1)	1.88 (10)	2.74 (3)
χ_{cc}, MHz	1.57 (1)	1.55 (10)	2.74 (3)

[a] Centrifugal distortion constants (kHz): D_J = 0.84 (4), D_{JK} = −0.79 (7), D_K = 4 (1). [b] Data from ref 15 and 16.

Table II. Structural Parameters of TMA·SO_2

	I[a]	II[a]	III[a]	Kraitchman[b]
d(N–S), Å	2.25	2.25	2.29	
α, deg	17.2	17.5	20.3	
β, deg	90.9	90.8	90.9	
$\lvert a_s \rvert$, Å	1.168	1.164	1.156	1.147
$\lvert c_s \rvert$, Å	0.367	0.374	0.386	0.430
ΔI,[c] amu·Å^2	0.570	0.038	0.032	

[a] Least-square fitting of observed moments and assumptions described in text. [b] Kraitchman substitution coordinates.[17] [c] $\Delta I = (I_{obsd} - I_{calcd})$ rms.

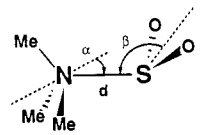

The N–S distance and the tilt angles α and β relative to the N–S distance can be estimated from the inertial parameters; however, some ambiguities are encountered. The ab initio structures and the observed selection rules suggest an *ac* symmetry plane which passes through N, S, and one C atom. This is confirmed by the agreement in $I_a + I_c - I_b$ for the two isotopic species (Table I), which should be invariant for substitution in this plane. The observed value of $I_a + I_c - I_b$ is 1.65 amu·Å^2 larger than calculated from the undistorted structures of free TMA and SO_2,[15,16] suggesting either a distortion of one or both subunits or a large amplitude internal motion.

There are other indications that a change in subunit(s) geometry should be considered, unlike hydrogen-bonded or van der Waals dimers in which the component structures remain virtually unchanged. The decrease in the quadrupole coupling constants from TMA seem too large to arise entirely from a large amplitude motion; for example, the change in χ_{bb} would imply an average out-of-plane bending amplitude of nearly 26°. These sizeable changes might imply an electronic redistribution which could affect the subunit geometries. The appreciable shifts in SO_2 vibrational frequencies[7] and the large dipole moment of the complex (4.60 D[6]) also suggest possible geometric changes in the subunits.

To estimate the N–S distance and the tilt angles α and β we adopt three strategies. (1) The TMA and SO_2 structures are fixed at the free molecule geometries, and their orientations adjusted in a least-squares fit to the moments of inertia of both species. This gives a poor fit since $I_a + I_c - I_b$ cannot match the experimental value (see above). (2) The S–O bonds are lengthened by 0.012 Å to match the observed $I_a + I_c - I_b$, repeating the least-squares fit. (3) The C–N–C angles in TMA are increased by 1.5° to match $I_a + I_c - I_b$ (SO_2 unchanged), and the least-squares fit is repeated. The results are listed in Table II along with a com-

(1) Dedicated to Prof. Milton Tamres upon appointment to Professor Emeritus status.
(2) Tamres, M. *Molecular Complexes*; Foster, R.; Ed.; Crane, Russak: New York, NY, 1973; Vol. 1, pp 49–116.
(3) Grundnes, J.; Christian, S. D.; Cheam, V.; Farnham, S. B. *J. Am. Chem. Soc.* **1971**, *93*, 20.
(4) Christian, S. D.; Grundnes, J. *Nature (London)* **1967**, *214*, 1111.
(5) Grundnes, J.; Christian, S. D. *J. Am. Chem. Soc.* **1968**, *90*, 2239.
(6) Moede, J. A.; Curran, C. *J. Am. Chem. Soc.* **1949**, *71*, 852.
(7) Sass, C. S.; Ault, B. S. *J. Phys. Chem.* **1984**, *88*, 432.
(8) Lucchese, R. R.; Haber, K.; Schaefer III, H. F. *J. Am. Chem. Soc.* **1976**, *98*, 7617.
(9) Douglas, J. E.; Kollman, P. A. *J. Am. Chem. Soc.* **1978**, *100*, 5226.
(10) Van der Helm, D.; Childs, J. D.; Christian, S. D. *Chem. Commun.* **1969**, 887.
(11) (a) Kollman, P. A. *Acc. Chem. Res.* **1977**, *10*, 365. (b) Singh, U. C.; Kollman, P. A. *J. Chem. Phys.* **1984**, *80*, 353.
(12) Hillig II, K. W.; Matos, J.; Scioly, A.; Kuczkowski, R. L. *Chem. Phys. Lett.* **1987**, *133*, 359.
(13) Balle, T. J.; Flygare, W. H. *Rev. Sci. Instr.* **1981**, *52*, 33.
(14) Burg, A. B. *J. Am. Chem. Soc.* **1943**, *65*, 1629.
(15) Harmony, M. D.; Laurie, V. W.; Kuczkowski, R. L.; Schwendeman, R. H.; Ramsay, D. A.; Lovas, F. J.; Lafferty, W. J.; Maki, A. G. *J. Phys. Chem. Ref. Data* **1979**, *8*, 619.
(16) Lide, D. R.; Mann, D. E. *J. Chem. Phys.* **1958**, *28*, 572.

0002-7863/87/1509-7222$01.50/0